Non-contrast enhanced non-invasive detection and follow-up of lung tumors in mice

Andrea Bianchi[1], Sandrine Dufort[2,3], Pierre-Yves Fortin[1,4], François Lux[5], Gerard Raffard[1], Nawal Tassali[1], Olivier Tillement[5], Jean-Luc Coll[2], and Yannick Crémillieux[1]

[1]Centre de Résonance Magnétique des Systèmes Biologiques, University of Bordeaux, Bordeaux, Bordeaux, France, [2]IAB-INSERM U823, University Joseph Fourier, Grenoble, France, [3]Nano-H, Saint Quentin – Fallavier, France, [4]Institut de Bio-Imagerie (IBIO) CNRS/UMS 3428, University of Bordeaux, Bordeaux, France, [5]ILM UMR 5306, University Lyon 1, Lyon, France

Introduction: Lung cancer is the leading cause of cancer deaths worldwide. One of the main reasons for the dismal prognosis of lung cancer is related to the late diagnosis of this pathology [1]. In this context, MRI can play a major role being a noninvasive imaging technique, characterized by good soft tissue contrast, high spatial resolution, and absence of ionizing radiation. We propose here an *in vivo* MRI longitudinal study of lung adenocarcinoma detection in tumor-bearing immunodeficient mice *without the use of contrast agents*. Free-breathing Ultra-short Echo Time (UTE) MRI acquisitions were compared to standard gradient echo lung MR images using both respiratory-gated and free-breathing protocols. The results were validated against Bioluminescence Imaging (BLI) and histology.

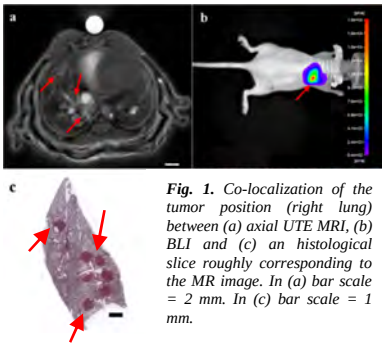

Fig. 1. *Co-localization of the tumor position (right lung) between (a) axial UTE MRI, (b) BLI and (c) an histological slice roughly corresponding to the MR image. In (a) bar scale = 2 mm. In (c) bar scale = 1 mm.*

Material and methods: Study protocol: Female NMRI immunodeficient mice (6 week-old, 24.0 ± 0.5 g) were used in the experiment. At day 0, an orthotopic implantation of H358-Luc bioluminescent tumor cells (10^6 cells/mouse) was performed in mice lungs (n=11) through an intratracheal administration. Three mice did not undergo the instillation and were left as controls. Animals were imaged with BLI at day 30 to study the tumor progression. A subgroup of mice (n=4) and controls were imaged with MRI at days 35, 43 and 51 to study the evolution of the tumor (follow-up study). The remaining mice (n=7) were imaged at days 35 and 37 to study the reproducibility of the measurement and the co-localisation between MRI, BLI and histology. After the acquisition of the last images, animals were sacrificed and lungs extracted to perform histology according to Ref. [2], roughly preserving the spatial information. MRI Protocol: Images were acquired with a 4.7 T Biospec spectrometer (Bruker, Ettlingen, D), using a transmitter/receiver quadrature coil of 25 mm inner diameter. For each animal 10 axial slices of the lungs of 1 mm thickness were acquired. The acquisition was performed in *freely-breathing* animals, using a 2D Ultra-Short Echo Time sequence (804 directions/128 points, 4 averages) with a TE of 276 µs, FOV of 3x3 cm, TR of 140 ms and FA of 60 degrees, for a total acquisition time of about 7 minutes. Similarly for each animal, 2D multislice FLASH was performed in freely breathing animals, using a matrix size 256 x 256, 4 averages, TR of 140 ms, TE of 2.5 ms, FA of 60 degrees, using the same geometry employed for the UTE images acquisition. The total acquisition time was of about 3 minutes. The same FLASH sequence, parameters, and geometry were used to perform an acquisition synchronized on the expiration phase of mice respiration. The total acquisition time was variable according to the respiration of the animals but roughly on the same order of the UTE acquisitions (7-8 minutes). MR image analysis: Following the procedure described in Ref [2], the signal-to-noise ratio (SNR) in the lung tumor was computed for each animal. In addition, the contrast-to-noise ratio (CNR) between the signal in tumor tissues and healthy tissues was computed. The total tumor volumes were computed according to the protocol in Ref. [2]. Data between different groups were compared using nonparametric Friedman test with a 0.05 significance level. BLI imaging: Five minutes after intraperitoneal injection of luciferin (150 µg/g), the mice were anesthetized and bioluminescence images and black-and-white pictures were acquired using a back-thinned CCD camera at -80°C (ORCAII-BT-512G, Hamamatsu, Massy, F). The intensity of tumor BLI signal (approximately proportional to the number of tumor cells) was measured and correlated to the tumor volume measured with MRI [2, 3] using a Spearman correlation coefficient.

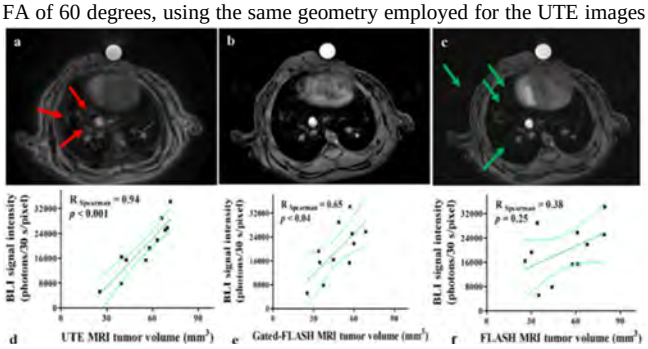

Fig. 2. *Axial slices obtained with MRI on the same tumor-bearing mouse using (a) non-gated UTE, (b) respiration-gated FLASH and (c) non-gated FLASH sequences. In (d-f) the correlation plot between the BLI signal intensity in tumor-bearing mice and MRI tumor volume is shown for (d) UTE, (e) gated-FLASH and (f) non-gated FLASH images.*

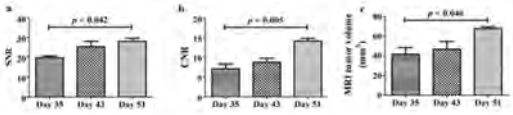

Fig. 3. *Bar plots of the (a) SNR, (b) CNR and (c) volume of the tumor, measured at three different time points using UTE MR images.*

Results: In all the mice a good co-localization was found between UTE MR images, bioluminescence images, and histology (*Fig. 1*). The two observers' identification of the presence of the tumor in MRI UTE slices was concordant in 94.3% of the cases. A typical comparison between axial slices obtained with non-gated UTE, respiratory-gated FLASH and non-gated FLASH sequences is shown in *Fig. 2*. Non-gated gradient-echo sequences presented a significant number of motion artifacts (*green arrows in Fig. 2c*). These artifacts appeared with the same signal intensity as tumor lesions and minor vessels, which made difficult to determine whether a tumor was present. Artifacts were consistently reduced in respiratory-gated FLASH images and negligible in non-gated UTE radial acquisitions. UTE images, as shown in *Fig. 2a with red arrows*, presented more extended tumor borders which were not identifiable with gated FLASH sequences. The extent of the tumor as verified with histological analysis confirmed the large infiltration of tumor cells in the lung tissue, as observed with non-gated UTE acquisitions. The total tumor volumes quantified with UTE MRI excellently correlated with the measured bioluminescent signal ($R = 0.94$, $p < 0.001$), as shown in *Fig. 2d*. The correlation was still significant when the quantification was performed using respiration-synchronized FLASH images ($R = 0.65$, $p = 0.034$, *Fig. 2e*). On the contrary, no significant correlation was found between the tumor volumes quantified with non-gated MRI FLASH images and the measured bioluminescence signal ($R = 0.38$, $p = 0.244$, *Fig. 2f*). The mice which were imaged at three different time points (days 35, 43, 51) showed a progressive increase of the tumor SNR and CNR (*Fig. 3a,b*), as well as a significant increase of tumor volume (*Fig.3c*). The signal-to-noise and contrast-to-noise ratios measured in the tumor at days 35 and 51 were significantly different ($p = 0.042$ and $p = 0.005$). Similarly, the volume of the tumors measured in the mice showed a significant increase from day 35 to day 51 ($p = 0.046$). Contrastingly, the SNR ($p = 0.552$), CNR ($p = 0.844$) and volume ($p = 0.513$) measured at two-day interval (days 35 and 37) were statistically identical.

Discussion: In this work, high-resolution MRI was employed to differentiate mice with lung neoplastic lesions from healthy animals while bioluminescence imaging and standard histological analyses were used to validate the MRI results. Several motion artifacts were observed in free-breathing gradient-echo acquisitions. As a consequence, the identification of the tumor tissue was difficult and strongly dependent on the artifacts of each non-gated FLASH image, as confirmed by the absence of a significant correlation between MRI-based tumor volume quantification and BLI-based measurements of orthotopic tumor growth. On the contrary, the motion artifacts were significantly reduced in the images acquired with the gated-FLASH sequence and negligible in UTE images. As a result, neoplastic lesions were satisfactorily identified and contoured on gated-FLASH and UTE images. The excellent correlation of the number of recorded photons and the MRI tumor volume measurements suggests that the segmentation procedure performed on UTE MR images is precise and accurate, further confirming the feasibility of proper noninvasive identification of tumor lesions made possible by the proposed method. The lower Spearman correlation coefficient obtained with gated-FLASH compared to UTE sequence images can probably be partially attributed to residual motion artifacts which can be erroneously computed as tumor tissues during the segmentation procedure. In addition, the UTE sequence provided a significantly lower TE compared to the FLASH acquisition, thus increasing the sensitivity for tumor detection.

Conclusion: In conclusion, the results presented in this work show that high-resolution MRI is a powerful imaging tool able to detect, quantify and longitudinally monitor the development of sub-millimetric non-small-cell lung cancers without the need of contrast agents. The data presented, validated with high-sensitivity bioluminescence imaging and conventional histopathologic analysis, clearly show the potential of radial UTE MRI in *in vivo* pre-clinical longitudinal studies, including testing of new chemotherapeutic drugs or investigation of oncogenic mechanisms. To our knowledge, this is the first study which proves the feasibility of a completely noninvasive MRI quantitative detection of lung adenocarcinoma in *freely breathing* mice *without the use of contrast agents.* The absence of ionizing radiation and high-resolution of MRI, along with the complete noninvasive nature and good reproducibility of the proposed non-gated protocol, make this imaging tool ideal for direct *translational applications*.

References: [1] *N Engl J Med*, 2008, 359:1367-80 [2] *PNAS, 2014*, 111(25):9247-52 [3] *Neoplasia*, 2000, 2(6):491-495

Acknowledgments: This work was supported by the European Marie Curie Action PI-NET-2010-264864 and the ANR project Gd-Lung ANR-12-P2 N-0009.